ESD-TR 70-195

Report No. 70-10

June 1970

LINEARLY POLARIZED ARRAYS WITH ALMOST ISOTROPIC RADIATION PATTERNS

H. S. CABAYAN
G. A. DESCHAMPS

Prepared by

Antenna Laboratory
Department of Electrical Engineering
University of Illinois
Urbana, Illinois

For

Massachusetts Institute of Technology
Lincoln Laboratory

Report No. 70-10
June 1970

LINEARLY POLARIZED ARRAYS WITH ALMOST ISOTROPIC RADIATION PATTERNS

H. S. CABAYAN

G. A. DESCHAMPS

Prepared by

Antenna Laboratory
Department of Electrical Engineering
University of Illinois
Urbana, Illinois

For

Massachusetts Institute of Technology
Lincoln Laboratory

Under

Purchase Order No. CC-401
Prime Contract No. AF 19(628)-5167

This work was partially supported by NSF Grant GK 2120.

UILU-ENG-70-308

ABSTRACT

A linearly polarized antenna cannot radiate power uniformly in all directions. However, by controlling the aperture excitation, as is done in an array, it is possible to reduce the maximum gain and approach conditions for isotropic radiation. A numerical method is presented which generates a family of designs which depend on a parameter α. As α approaches zero, the radiation pattern tends to become more isotropic. However, the efficiency is reduced and the sensitivity of the pattern to errors in the aperture function is increased. In some cases this sensitivity is so high as to make the result worthless. The design, therefore, must be a compromise between closeness to conditions of isotropic radiation on one hand, and losses and sensitivity to errors on the other.

The sensitivity to errors, expressed by the pattern deterioration for a given level of error, has been evaluated by a numerical experiment (Monte Carlo method). A general relation has also been established between the sensitivity and the losses in the antenna. It agrees with the numerical experiment and can be used as a guide to choose the regularization parameter α.

Accepted for the Air Force
Franklin C. Hudson
Chief, Lincoln Laboratory Office

TABLE OF CONTENTS

LIST OF ILLUSTRATIONS

Figure Page

1. INTRODUCTION

A linearly polarized antenna cannot radiate power uniformly in all directions. This condition of isotropic radiation, or unity gain, is also impossible if one specifies the axial ratio of the polarization ellipse.[1] However, accepting the existence of nulls in the radiation pattern, one may ask if it is possible to reduce the total solid angle in which the gain falls below a certain level. This is equivalent to reducing the maximum gain.

It will be shown that it is, indeed, possible to make the maximum gain as close to unity as one wishes. However, the practical difficulties in doing this are the same as those encountered in trying to increase the gain of an antenna indefinitely. To reach a certain level of performance (gain or lack of gain), one must have an antenna of sufficient aperture. If, for a given aperture, we try to improve the performance above a certain level, we have to increase drastically the antenna currents (or the near field). As a consequence, both the losses and the sensitivity to construction errors are increased. This is characteristic of the supergain problem. It occurs more generally anytime one tries to shape a radiation pattern too accurately. In particular, it occurs in the "minimum gain" problem considered here.

The need for an isotropic radiator arises when one disposes of a certain amount of power and one wishes to produce a radiation intensity higher than a given level in a solid angle as large as possible. This may be for the purpose of reaching a target whose direction is not known a priori. Conversely, in the receiving case, one may want to receive a sufficient signal from a source of given power and unknown direction.

Although the method used could be generalized, we shall consider in this report a colinear array of dipoles as shown in Figure 1a. From the far-field power pattern of this antenna, which is shown in Figure 1b, and some gain level G_m, one can read the total solid angle Ω in which the gain falls below G_m. The plot of $G(\Omega)$ versus Ω is shown in Figure 1c. In this plot, $(4\pi-\Omega)$ is the total solid angle in which the gain exceeds G_m.

Given the curve $G(\Omega)$, the total available power P watts, and the desired radiation intensity I watts/steradian, the useful angle $(4\pi-\Omega)$ is defined by

$$\frac{P}{4\pi} G(4\pi-\Omega) = I$$

or

$$G(4\pi-\Omega) = \frac{4\pi I}{P} = G_m.$$

If the ratio I/P is small, Ω will be small for any design. However, when I/P is large, then special designs become necessary in order to produce an intensity I in as large a solid angle as possible.

In Figure 1c, the shaded portion under the gain curve has an area equal to 4π. The total area of the rectangles ABCD and DEFH exceeds that of the shaded portion. Accordingly, the following inequality may be written,

$$(4\pi-\Omega)G_M + \alpha G_m \geq 4\pi$$

or

$$\Omega \leq 4\pi\ (G_M-1)/(G_m-g),$$

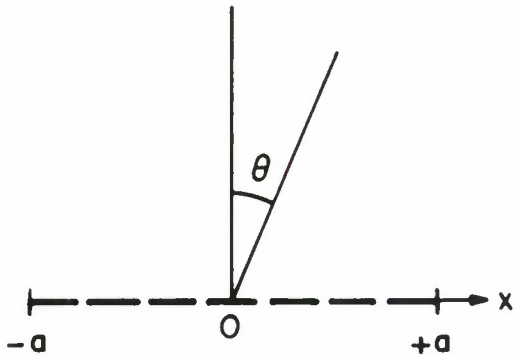

(a)

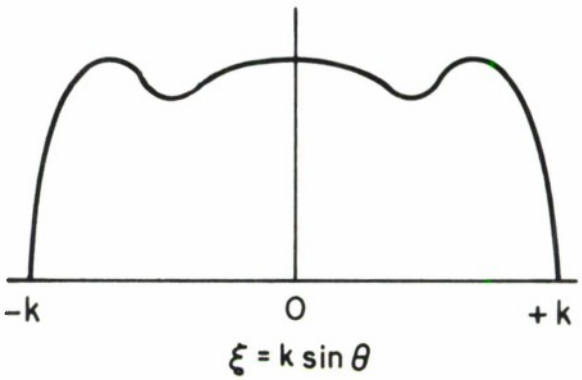

(b)

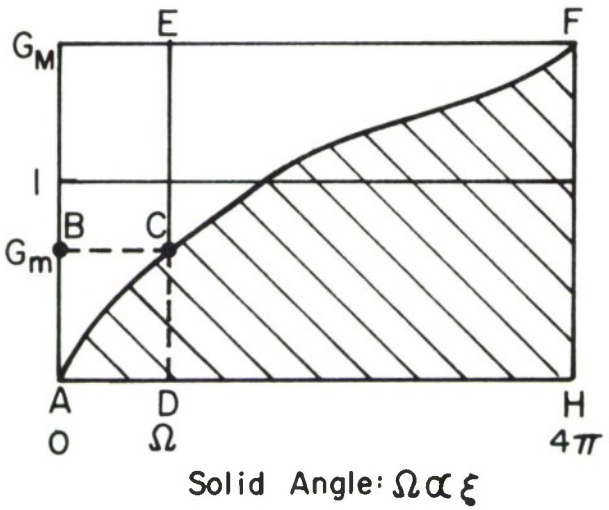

(c)

Figure 1. Schematic representation of array and its far-field gain and power patterns.
(a) Array of colinear dipoles.
(b) Far-field power pattern.
(c) Curve of gain versus solid angle.

where G_M is the maximum gain. This last inequality implies that for $\Omega \to 0$, the maximum gain G_M must approach unity.

To obtain an indication of what can be achieved practically with a moderately short antenna (1 wavelength), this report considers the synthesis of linear antenna arrays made of dipoles aligned in some direction, Ox, as shown in Figure 1a. The resulting pattern has nulls in the directions $\pm x$. The problem is to reduce the cones where the gain is below a certain level. A general method based on the concept of regularization[2,3] was developed in the Antenna Laboratory under NSF Grant GK 2120. It will be applied to the problem.

2. STATEMENT OF THE PROBLEM

The general case of a pattern function $g_0(\xi)$ defined over the visible region $[-k \leq \xi \leq k]$ will be first considered, and the numerical results will be specialized to the case

$$g_0(\xi) = 1 \quad [-k \leq \xi \leq k] \tag{1}$$

where the gain is equal to one over the whole visible region. A source distribution f(x) representing an array of N elements over the aperture $[-a \leq x \leq a]$ is of the form

$$f(x) = \sum_{n=1}^{N} f_n \delta(x-x_n). \tag{2}$$

The problem is to determine the $\{f_n\}$ such that the pattern function of the array comes close to $g_0(\xi)$.

The far-field pattern of a linearly polarized source f(x) is given by

$$g(\xi) = Tf = e(\xi) \int_{-a}^{a} f(x)e^{i\xi x}\, dx \quad [-k \leq \xi \leq k] \tag{3}$$

where $\xi = k \sin \theta$. The first factor $e(\xi)$ is the element pattern.

For a source distribution described in Equation (2), the far-field pattern is given by,

$$g(\xi) = Tf = \sum_{n=1}^{N} f_n g_n(\xi) \tag{4}$$

where

$$g_n(\xi) = e(\xi)e^{i\xi x_n} \quad [-k \leq \xi \leq k].$$

The function $g(\xi)$, therefore, belongs to a finite dimensional vector space $\mathcal{C}^N$ spanned by the N elements $g_n(\xi)$ $(1 \leq n \leq N)$. In general, $g_0(\xi)$ does not belong to this subspace and the problem is to determine the complex coefficients $\{f_n\}$ such that the pattern given by (4) comes close to $g_0(\xi)$.

In one method proposed in the next Chapter, the coefficients $\{f_n\}$ are determined such that the corresponding pattern $g(\xi)$ is the orthogonal projection of $g_0(\xi)$ on the finite dimensional subspace $\mathcal{C}^N$. This gives the least-squares approximation to $g_0(\xi)$.

This straightforward projection, however, may result in a solution with a high Q factor, that is, excitation currents $\{f_n\}$ that are very large for a given power radiated. These currents vary widely from element to element, and the resulting far-field pattern becomes very sensitive to errors in construction.

To avoid this difficulty in problems of the same type, Tihonov[2] has proposed a method of regularization which consists of imposing some restrictions on the acceptable solutions, that is,on the aperture functions f. The regularization algorithm depends on a parameter α such that for $\alpha = 0$, we have the direct projection on the subspace $\mathcal{C}^N$. As α increases, a set of solutions is obtained with decreasing values of the Q factor. This set of solutions invariably produces far-field patterns that are further away from the desired pattern but are also less subject to ohmic losses and less sensitive to errors in construction.

To give a precise meaning to the concept of projection and of Q factor, one has to introduce appropriate norms in the space $\mathcal{F}$ of source functions $f = \{f_n\}$ and the space $\mathcal{G}$ of far-field patterns $g(\xi)$. In both

spaces, it is natural to choose the L_2 norm which can be interpreted in the space $\mathcal{G}$ as the power radiated by the antenna. Thus,

$$||f||^2 = \sum_{n=1}^{N} f_n^* f_n \tag{5}$$

and

$$||g||^2 = \frac{1}{k} \int_{-k}^{+k} g^*(\xi)\, g(\xi)\, d\xi. \tag{6}$$

The Q factor for a given design is represented by

$$Q = ||f||^2 \,/\, ||g||^2. \tag{7}$$

Because of the element pattern, this factor is not always larger than one.

3. METHOD OF SOLUTION

Tihonov's procedure consists of minimizing the functional

$$J_\alpha^*(f;g_0) = ||g-g_0||^2 + \alpha||f||^2$$

$$= \frac{1}{k}\int_{-k}^{k} \left| \sum_{n=1}^{N} f_n g_n - g_0 \right|^2 d\xi + \alpha \sum_{n=1}^{N} |f_n|^2 \qquad (8)$$

where α is a positive constant referred to as the regularization parameter.

By setting the first variation of $J_\alpha(f;g)$ with respect to $f = \{f_n\}$ equal to zero, the following equation for $f_\alpha = \{f_{\alpha_n}\}$, the minimizing set of excitations, is obtained,

$$\sum_{n=1}^{N} f_{\alpha_n} \frac{1}{k}\int_{-k}^{k} g_n g_m^* d\xi + \alpha f_{\alpha_m} = \frac{1}{k}\int_{-k}^{k} g_0 \cdot g_m \, d\xi \qquad (1 \leq n, m \leq N)$$

where, since g_0 is symmetrical, the excitations $\{f_n\}$ are assumed real.

In matrix notation,

$$(G+\alpha I)f_\alpha = G_0\tilde{g}_0 \qquad (9)$$

where G is an (N x N) square matrix with terms G_{mn} given by

$$G_{mn} = \frac{1}{k}\int_{-k}^{k} e(\xi)e^*(\xi)e^{i\xi(x_n-x_m)} \, d\xi, \qquad (10)$$

and I is the identity matrix of dimension N.

The column matrix $g_0 = \{g_{0_j}\}$ $(1 \leq j \leq M)$ represents the sampled values of the function g_0 at the M equally spaced points over the

visible region [$-k \leq \xi \leq k$], and G_0 is a (N x M) quadrature matrix derived to perform numerically the integral

$$\frac{1}{k} \int_{-k}^{k} g_0 g_m^* \, d\xi$$

for any given function $g_0(\xi)$.

Equation (10) shows that the G_{mn} are the Fourier Transforms H(x) of $h(\xi) = |e(\xi)|^2$ evaluated for $x_n - x_m$.

$$G_{mn} = H(x_n - x_m).$$

When the elements are dipoles in the x direction,

$$e(\xi) = \cos\theta = \left(1 - \frac{\xi^2}{k^2}\right)^{1/2} \tag{11}$$

and

$$H(x) = 2\sqrt{(2\pi)} \, \frac{J_{3/2}(kx)}{(kx)^{3/2}}$$

$$= \frac{4}{(kx)^2} \left[\frac{\sin(kx)}{(kx)} - \cos(kx) \right]. \tag{12}$$

To derive the elements $G_{0_{ij}}$ of the Quadrature matrix G_0, the function g_0 is sampled at equally spaced points over the visible region [$k \leq \xi \leq k$] and approximated by straight lines over each interval. For the range,

$$\xi_{j-1} \leq \xi \leq \xi_j$$

$$g_0(\xi) \simeq \frac{1}{h} \left[g_j(\xi - \xi_{j-1}) - g_{j-1}(\xi - \xi_j) \right]$$

where h is the length of each interval. For the range,

$$\xi_j \leq \xi \leq \xi_{j+1}$$

$$g_0(\xi) \simeq \frac{1}{h}\left[g_{j+1}(\xi-\xi_j)-g_j(\xi-\xi_{j+1})\right]$$

and the terms $G_{0_{ij}}$ are given by

$$G_{0_{ij}} = \frac{1}{k}\frac{1}{h}\left\{\int_{\xi_{j-1}}^{\xi_j}(\xi-\xi_{j-1})\left(1-\frac{\xi^2}{k^2}\right)^{1/2}e^{i\xi x_i}d\xi - \int_{\xi_j}^{\xi_{j+1}}(\xi-\xi_{j+1})\left(1-\frac{\xi^2}{k^2}\right)^{1/2}e^{i\xi x_i}d\xi\right\}.$$

Since these integrals cannot be evaluated in closed form, they were evaluated by Simpson's three-point quadrature. From (9),

$$f_\alpha = (G+\alpha I)^{-1} G_0 \tilde{g}_0. \tag{13}$$

Once a choice for α is made, Equation (13) gives a unique solution f_α for a given g_0. This solution f_α has a far-field pattern g_α, given by

$$g_\alpha = Tf_\alpha \tag{14}$$

and a corresponding Q factor. The function f_α has the property that, for this value of Q, its far-field pattern g_α yields the least-squares fit to g_0.

4. NUMERICAL RESULTS

In order to study the relationship of α to the sensitivity of the design to errors, Equation (13) was solved for a number of values of α ranging from 0 to 10^{-1}.

The magnitudes of the element excitations for arrays of five and seven elements are reported in Tables I and II, respectively, for various values of the regularization parameter. The element pattern $e(\xi)$ is given in Equation (11).

TABLE I. MAGNITUDE OF ELEMENT EXCITATIONS FOR THE FIVE-ELEMENT ARRAY.

Element Number	$\alpha = 0$	$\alpha = 10^{-3}$	$\alpha = 10^{-2}$	$\alpha = 10^{-1}$
1	.64	.35	-.15	-.28
2	-2.25	-1.47	-.11	.335
3	4.28	3.26	1.47	.86
4	-2.25	-1.47	-.11	.336
5	.64	.35	-.15	-.28

The far-field pattern g_α corresponding to each solution f_α is evaluated using Equation (4). Since it is assumed that only power $P = ||g_0||^2$ is available to the array for radiation, the excitations $\{f_{\alpha_n}\}$ are normalized such that

$$||g_\alpha||^2 = ||g_0||^2 .$$

Let $\bar{f}_\alpha = \{\bar{f}_{\alpha_n}\}$ and $\bar{g}_\alpha$ be the normalized sources and far-field patterns, respectively. The relative error ε_α^2 due to regularization is expressed by the norm of the error $||\bar{g}_\alpha - g_0||^2$ divided by that of the desired

TABLE II. MAGNITUDE OF ELEMENT EXCITATION FOR THE SEVEN-ELEMENT ARRAY.

Element Number	$\alpha = 0$	$\alpha = 10^{-6}$	$\alpha = 10^{-5}$	$\alpha = 10^{-4}$
1	-6.71	-1.58	.57	.87
2	35.07	10.19	-.29	-1.80
3	-81.46	-26.53	-3.36	.07
4	107.20	36.88	7.22	2.79
5	-81.46	-26.53	-3.36	.07
6	35.07	10.19	-.29	-1.80
7	-6.71	-1.58	.57	.87

Element Number	$\alpha = 10^{-2}$	$\alpha = 10^{-1}$
1	.05	-.23
2	-.55	-.01
3	.43	.41
4	1.08	.62
5	.43	.41
6	.55	-.01
7	.05	-.23

pattern $||g_0||^2$

$$\varepsilon_\alpha^2 = ||\bar{g}_\alpha - g_0||^2 \; / \; ||g_0||^2$$

$$= \frac{1}{k} \int_{-k}^{k} |\bar{g}_\alpha - g_0|^2 \, d\xi \; / \; ||g_0||^2 \; . \qquad (15)$$

Next, in order to study the sensitivity of each design to errors in construction, a random relative error $\underline{\nu}$ is introduced to the source function, and these excitations with noise are denoted by $f_{\alpha\nu_n}$ and given by

$$f_{\alpha\nu_n} = \bar{f}_{\alpha_n} (1+\nu_n) \tag{16}$$

where $\underline{\nu} = \{\nu_n\}$ are random complex numbers with a Gaussian distribution

$$E(\nu_n) = 0$$

$$E(\nu_n {}^{*}\nu_m) = \nu^2 \delta_{nm}.$$

The far-field pattern corresponding to sources $\{f_{\alpha\nu_n}\}$ is denoted by $g_{\alpha\nu}$. The excitations $\{f_{\alpha\nu_n}\}$ are normalized such that $||g_{\alpha\nu}||^2 = ||g_0||^2$. Let $\bar{f}_{\alpha\nu} = \{\bar{f}_{\alpha\nu_n}\}$ and $\bar{g}_{\alpha\nu}$ be the normalized sources and far-field pattern, respectively. The relative error ε_{ν}^2, due to the introduction of random noise, is expressed by the norm of the error $||\bar{g}_{\alpha\nu}-g_\alpha||^2$ divided by that of the desired pattern.

$$\varepsilon_{\underline{\nu}}^2 = ||\bar{g}_{\alpha\nu}-\bar{g}_\alpha||^2 \; / \; ||g_0||^2, \tag{17}$$

and the corresponding relative errors due to regularization and the introduction of random noise are expressed by the norm of the error $||\bar{g}_{\alpha\nu}-g_0||^2$ divided by $||g_0||^2$:

$$\varepsilon_t^2 = ||\bar{g}_{\alpha\nu}-g_0||^2 \; / \; ||g_0||^2.$$

For each design, the Q-factor is calculated with the presence of random errors and denoted by $Q_{\underline{\nu}}$, where

$$Q_{\underline{\nu}} = ||\bar{f}_{\alpha\nu}||^2 \; / \; ||\bar{g}_{\alpha\nu}||^2. \tag{18}$$

In each instance, 25 sets of random errors were introduced and the average of the quantities $\varepsilon_{\underline{\nu}}^2$, ε_t^2, and $(1/Q_{\underline{\nu}})$ were calculated over the 25 trials, where

$$\varepsilon_\nu^2 = \langle \varepsilon_{\underline{\nu}}^2 \rangle_{av}$$

$$\overline{\varepsilon_t^2} = \langle \varepsilon_t^2 \rangle_{av} \tag{19}$$

$$1/Q_\nu = \langle 1/Q_{\underline{\nu}} \rangle_{av}.$$

The quantities ε_α, $\varepsilon_{\underline{\nu}}$, and ε_t are illustrated schematically in Figure 2. In this diagram, vectors are understood to represent functions and straight lines, distances in the sense of the L_2 norm. The curved lines represent operators mapping the space of source functions into the space of far-field pattern functions. The three vectors g_0, $\bar{g}_\alpha$, and $\bar{g}_{\alpha\nu}$ are drawn with their tips on the same circle to indicate that their L_2 norms are equal.

The far-field power patterns $\|\bar{g}_\alpha\|^2$ and $|\bar{g}_{\alpha\nu}|^2$ of the arrays for various values of the regularization parameter α are shown in Figures 3 to 11. Also in the same figures, the power pattern intensity of an elementary dipole is shown for comparison. The horizontal line drawn for a radiation intensity = 1 is that of an ideal isotropic radiator. It is pointed out again that all pattern functions are normalized such that their L_2 norms are equal. This makes their radiated power, represented by the area under the curve, equal in all cases. In Figures 12 and 13, curves for the quantities ε_α^2, ε_ν^2, $\overline{\varepsilon_t^2}$ and Q are shown as a function of the regularization parameter α for the arrays of five elements and seven elements, respectively.

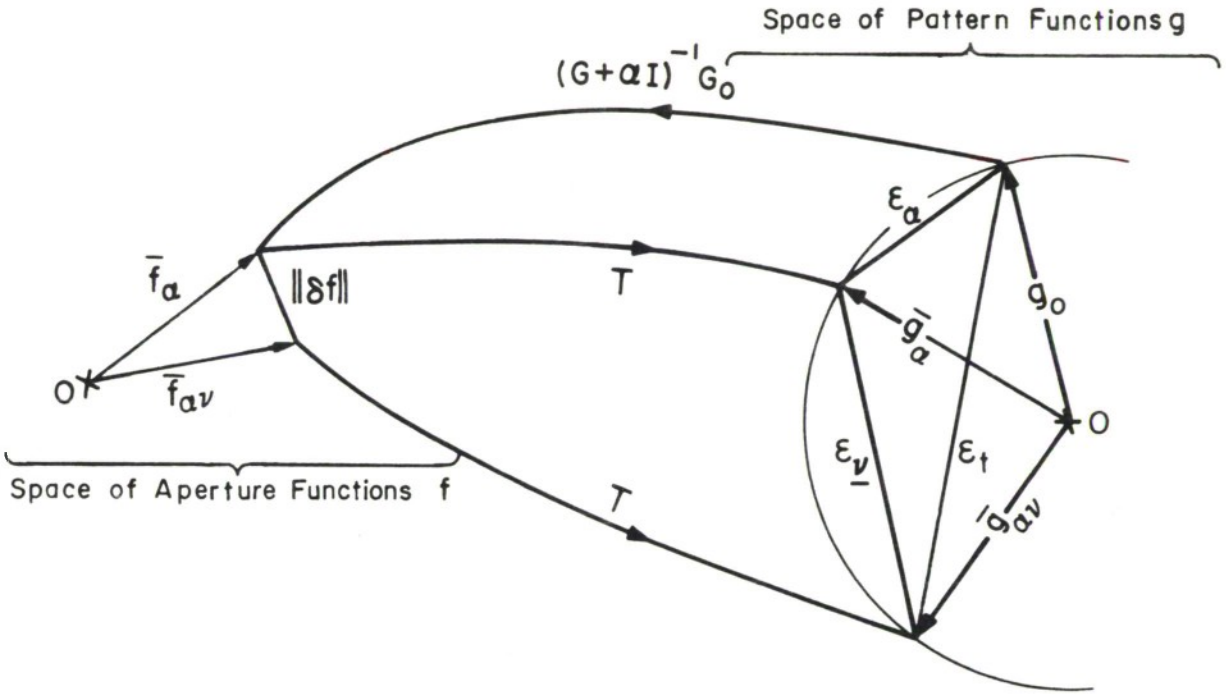

Figure 2. Schematic representation of the quantities ε_α, ε_ν, and ε_t.

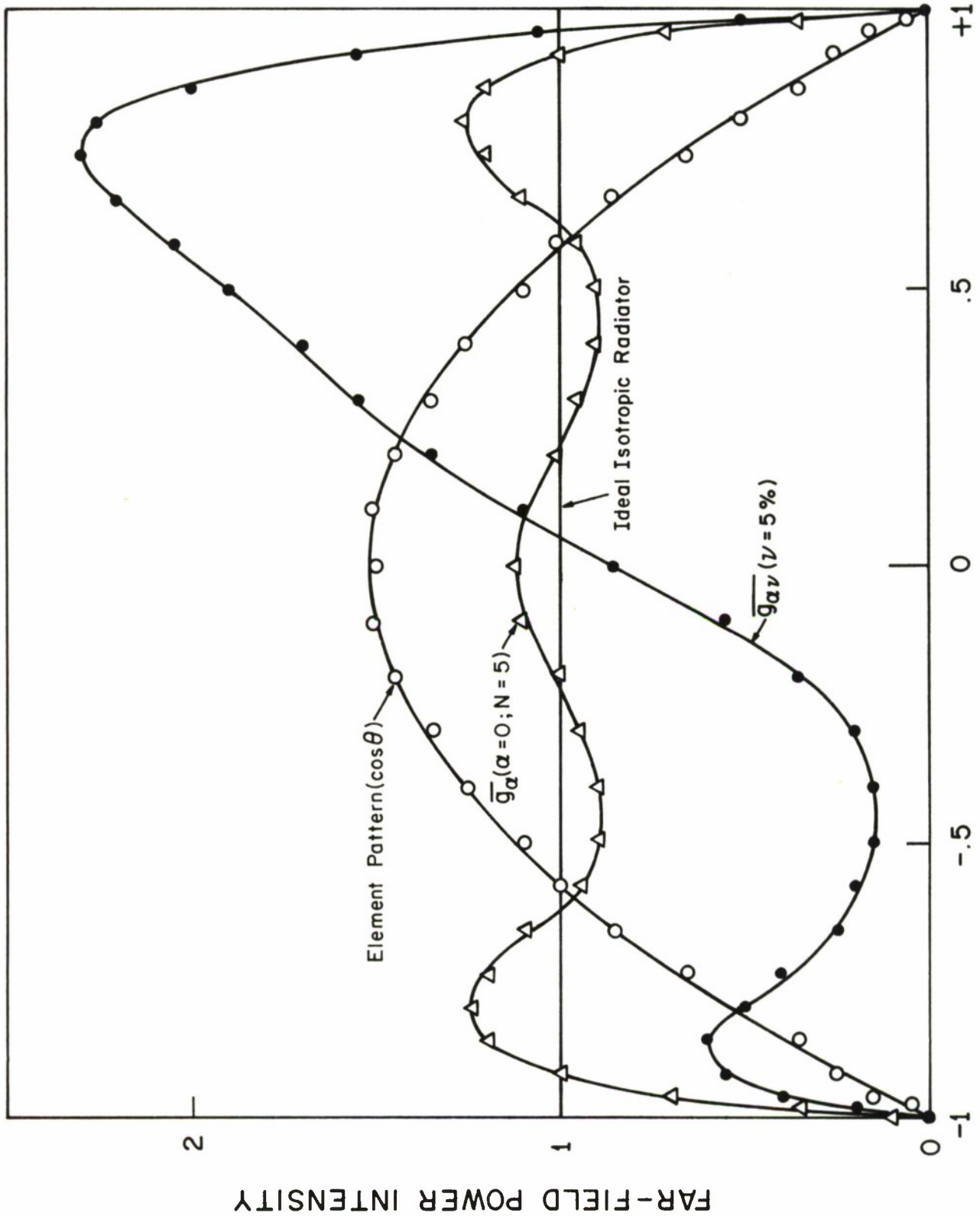

Figure 3. Far-field power intensity patterns $|\bar{g}_\alpha|^2$ and $|\bar{g}_{\alpha\nu}|^2$ for the case N = 5 and $\alpha = 0$.

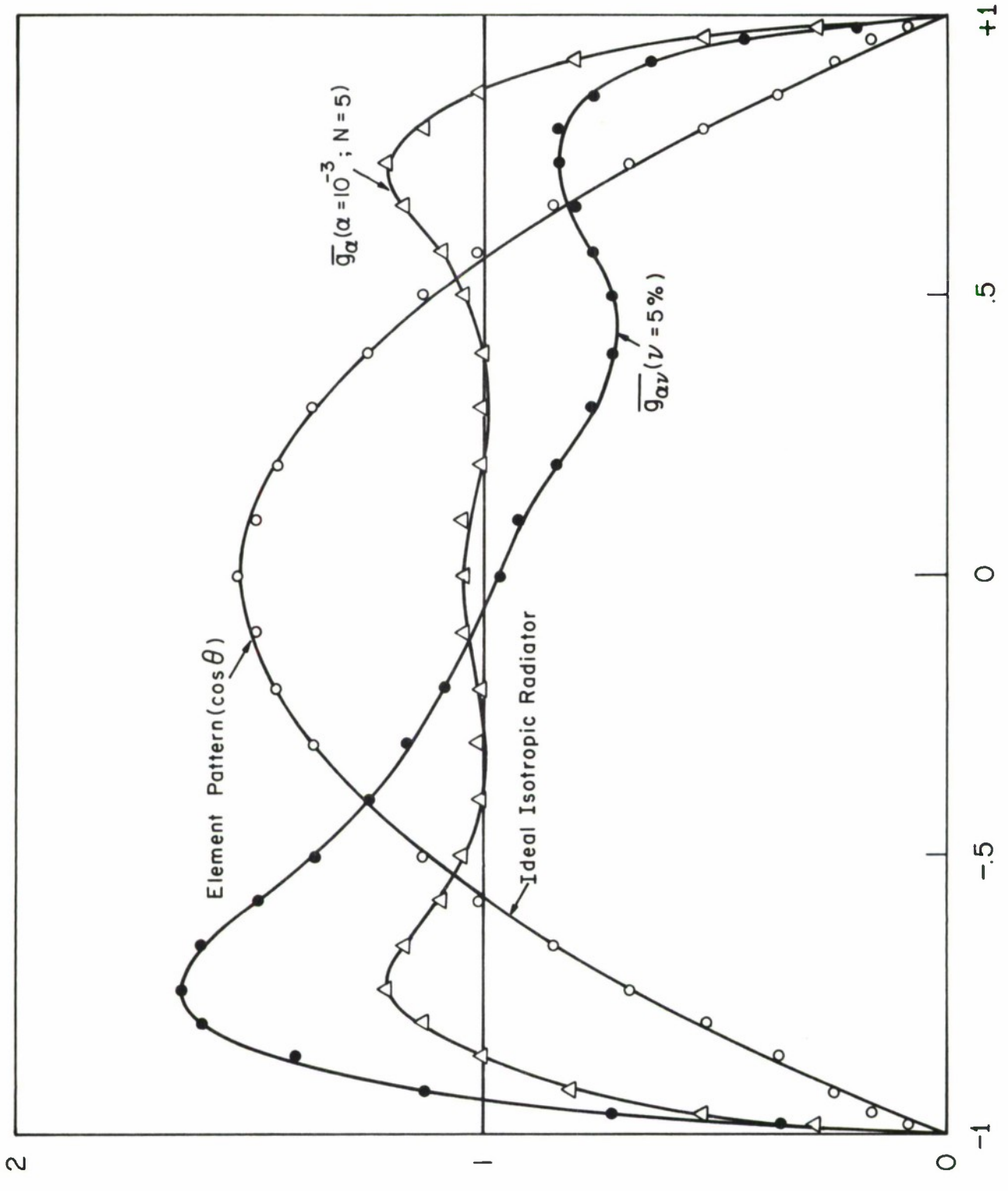

Figure 4. Far-field power intensity patterns $|\overline{g_\alpha}|^2$ and $|g_{\alpha\nu}|^2$ for the case N = 5 and $\alpha = 10^{-3}$.

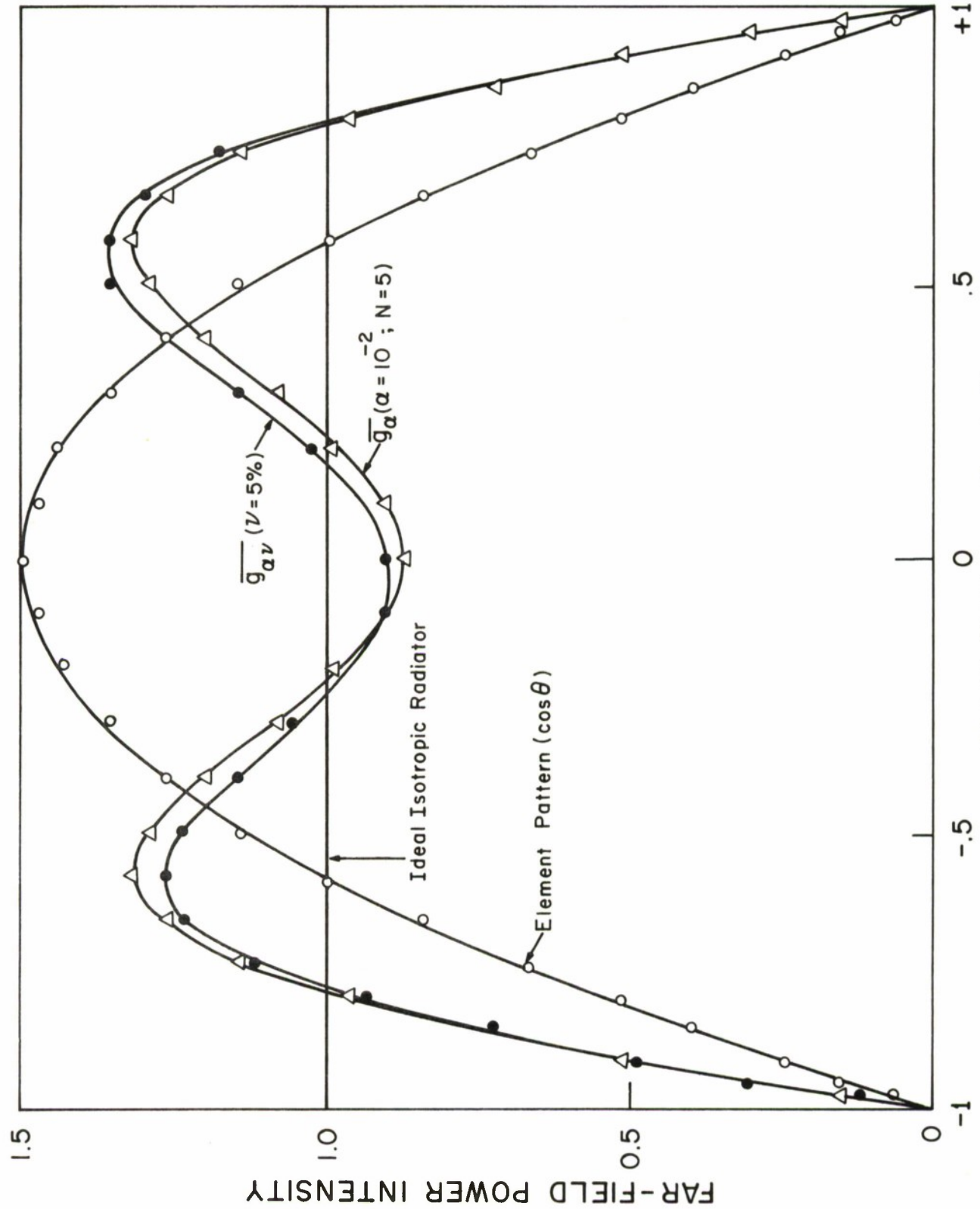

Figure 5. Far-field power intensity patterns $|\bar{g}_\alpha|^2$ and $|\bar{g}_{\alpha\nu}|^2$ for the case N = 5 and $\alpha = 10^{-2}$.

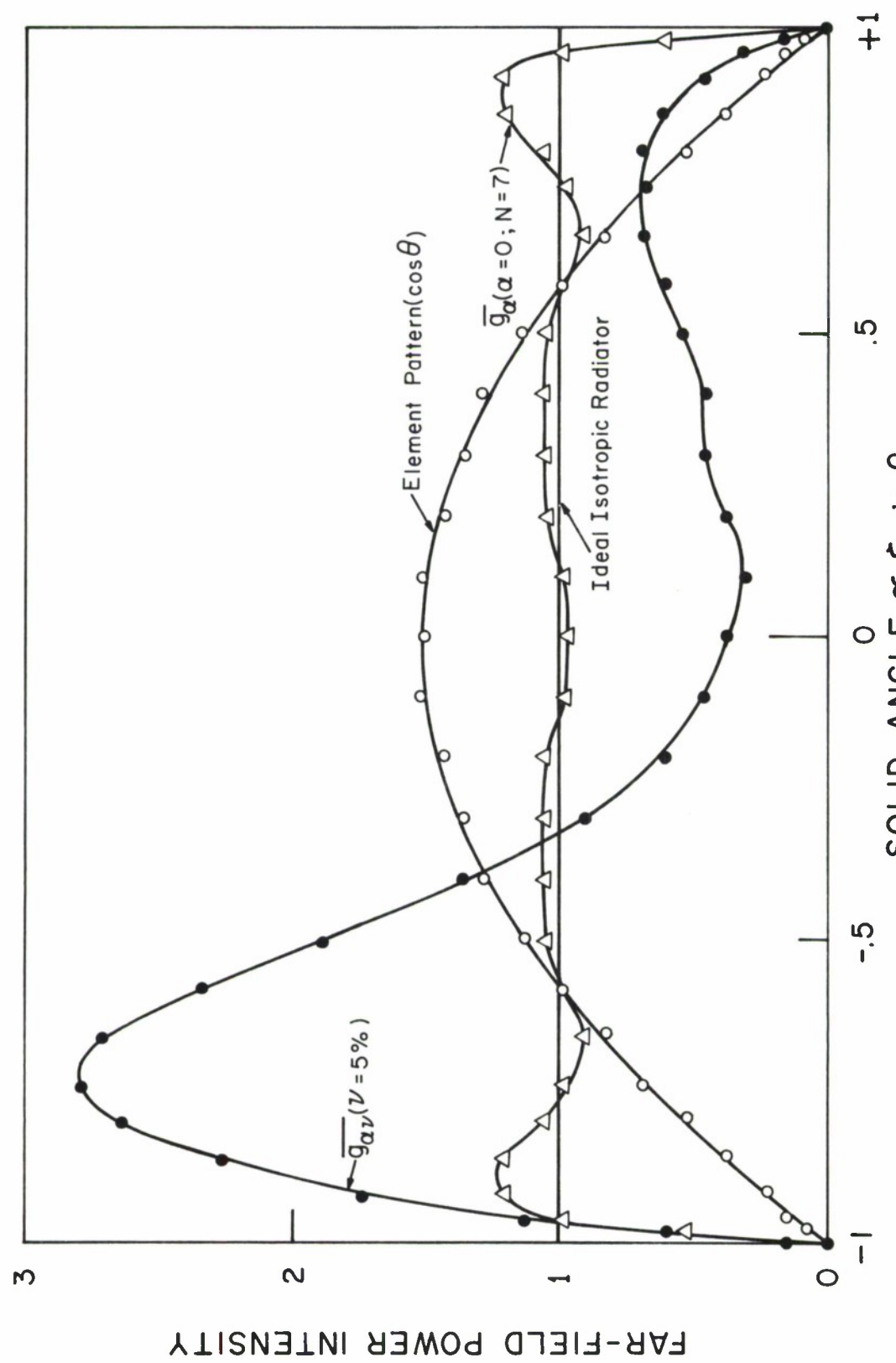

Figure 6. Far-field power intensity patterns $|\bar{g}_{\alpha}|^2$ and $|\bar{g}_{\alpha\nu}|^2$ for the case N = 7 and α = 0.

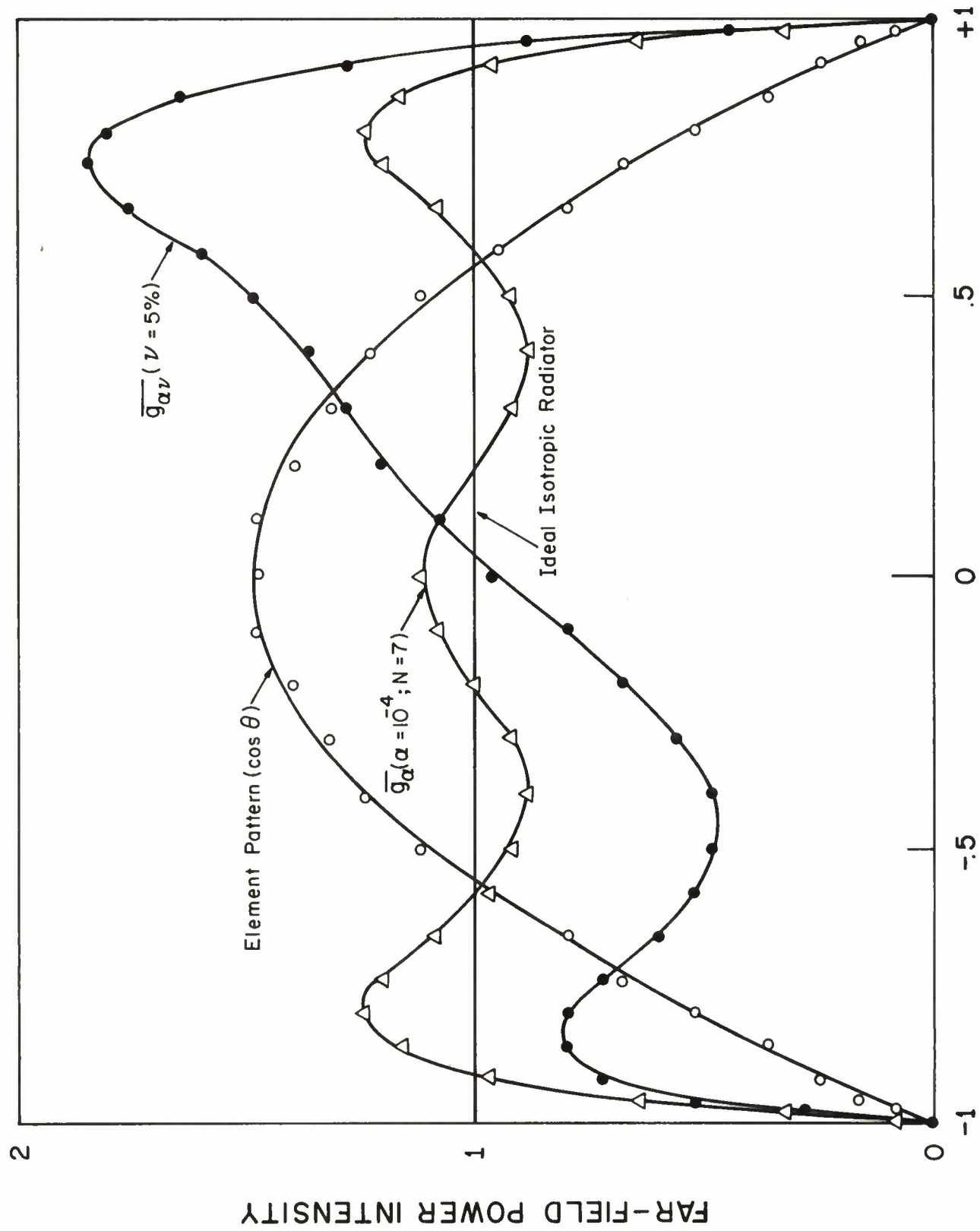

Figure 7. Far-field power intensity patterns $|\bar{g}_\alpha|^2$ and $|\bar{g}_{\alpha\nu}|^2$ for the case N = 7 and $\alpha = 10^{-5}$.

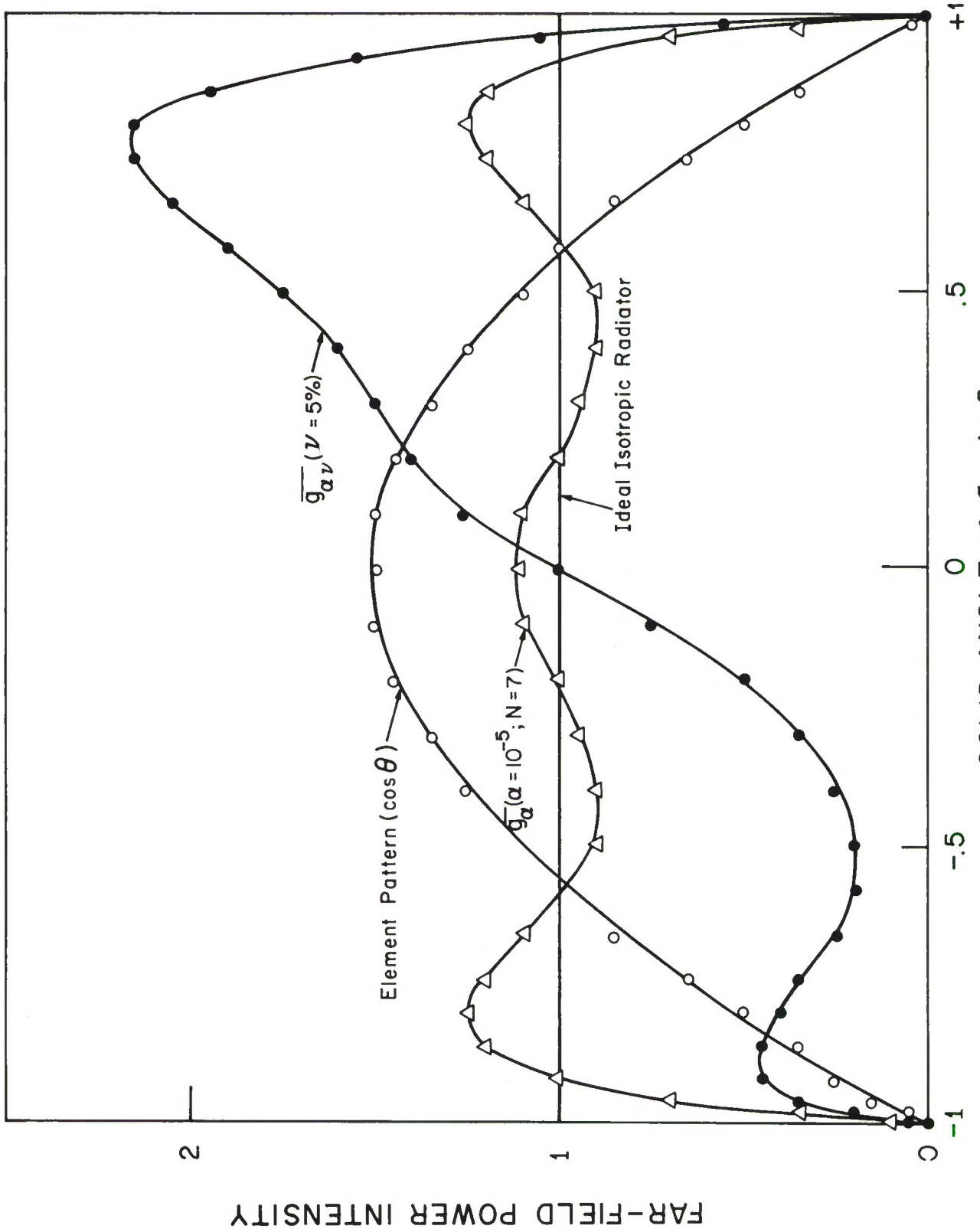

Figure 8. Far-field power intensity patterns $|\bar{g}_\alpha|^2$ and $|\bar{g}_{\alpha\nu}|^2$ for the case N = 7 and $\alpha = 10^{-4}$.

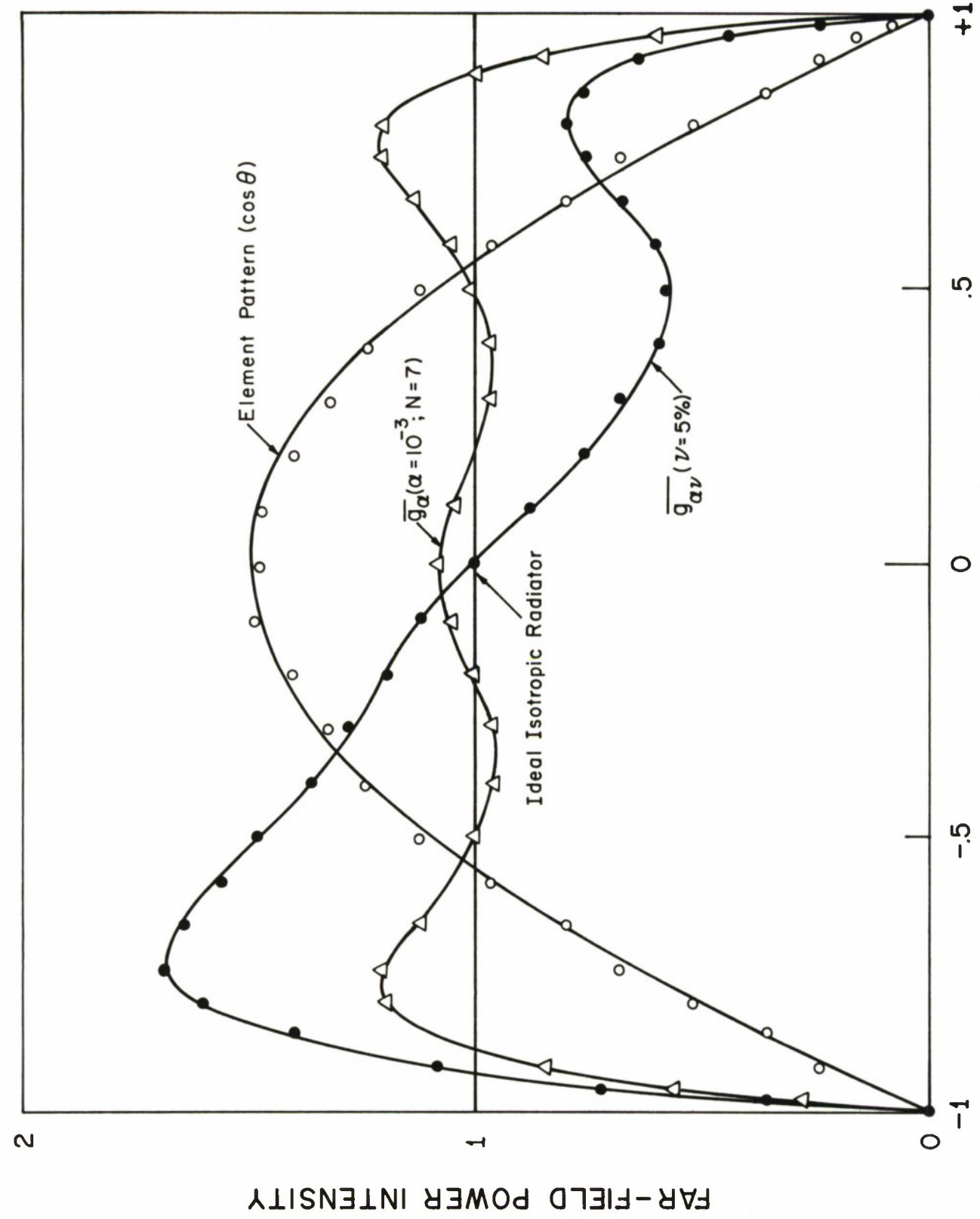

Figure 9. Far-field power intensity patterns $|\bar{g}_\alpha|^2$ and $|\bar{g}_{\alpha\nu}|^2$ for the case N = 7 and $\alpha = 10^{-3}$.

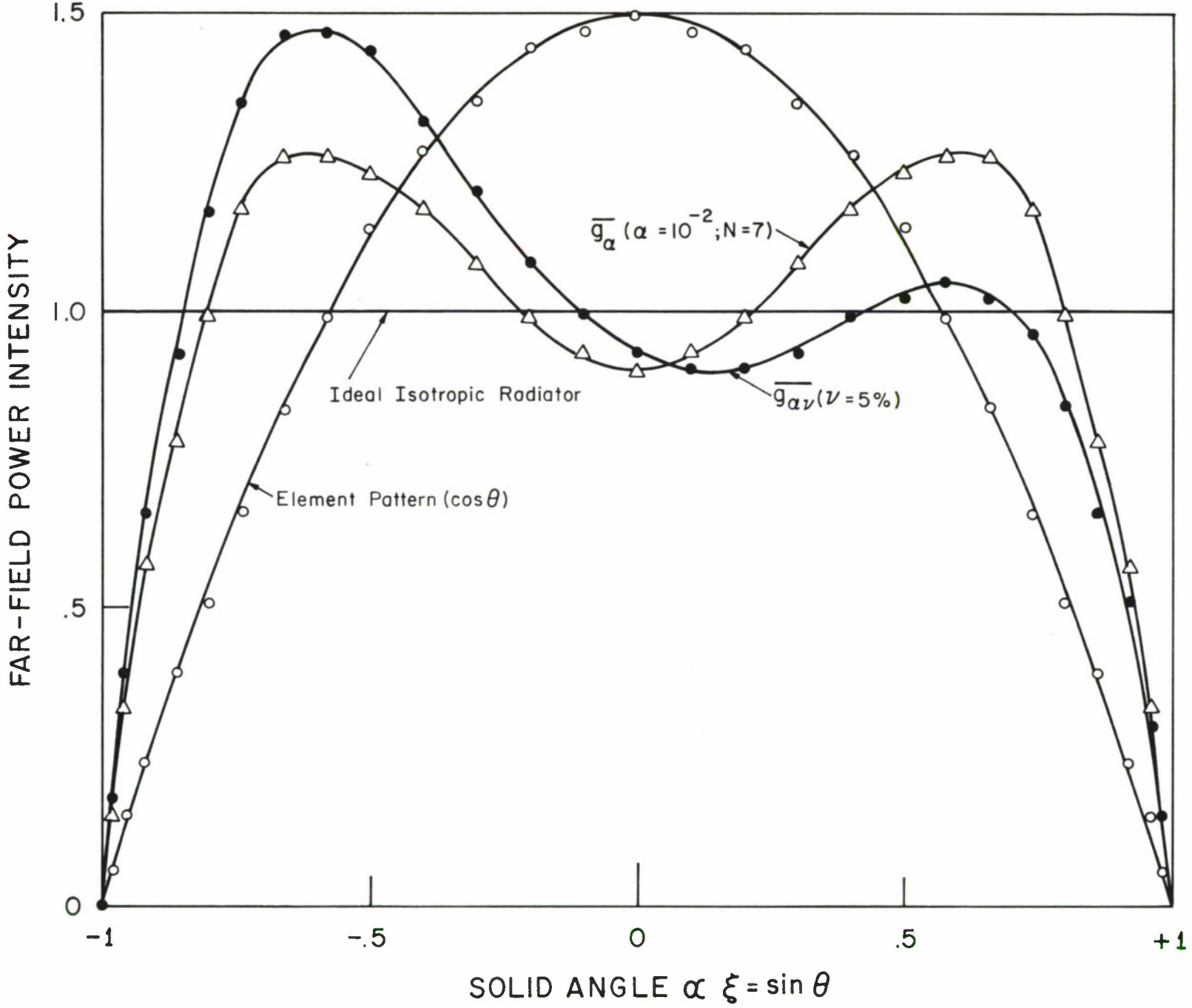

Figure 10. Far-field power intensity patterns $|\bar{g}_\alpha|^2$ and $|\bar{g}_{\alpha\nu}|^2$ for the case N = 7 and $\alpha = 10^{-2}$.

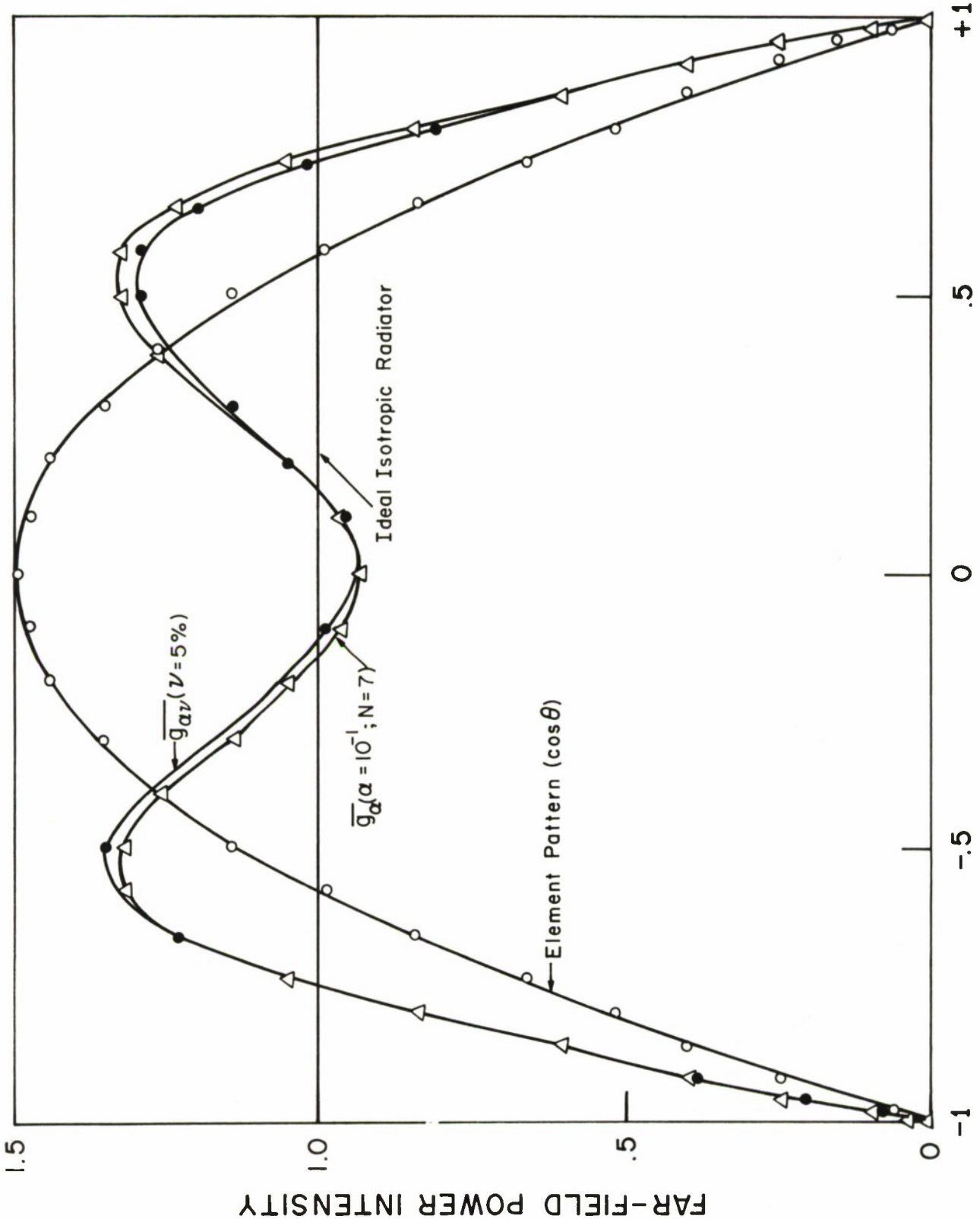

Figure 11. Far-field power intensity patterns $|\tilde{g}_{\alpha}|^2$ and $|\tilde{g}_{\alpha\nu}|^2$ for the case N = 7 and $\alpha = 10^{-1}$.

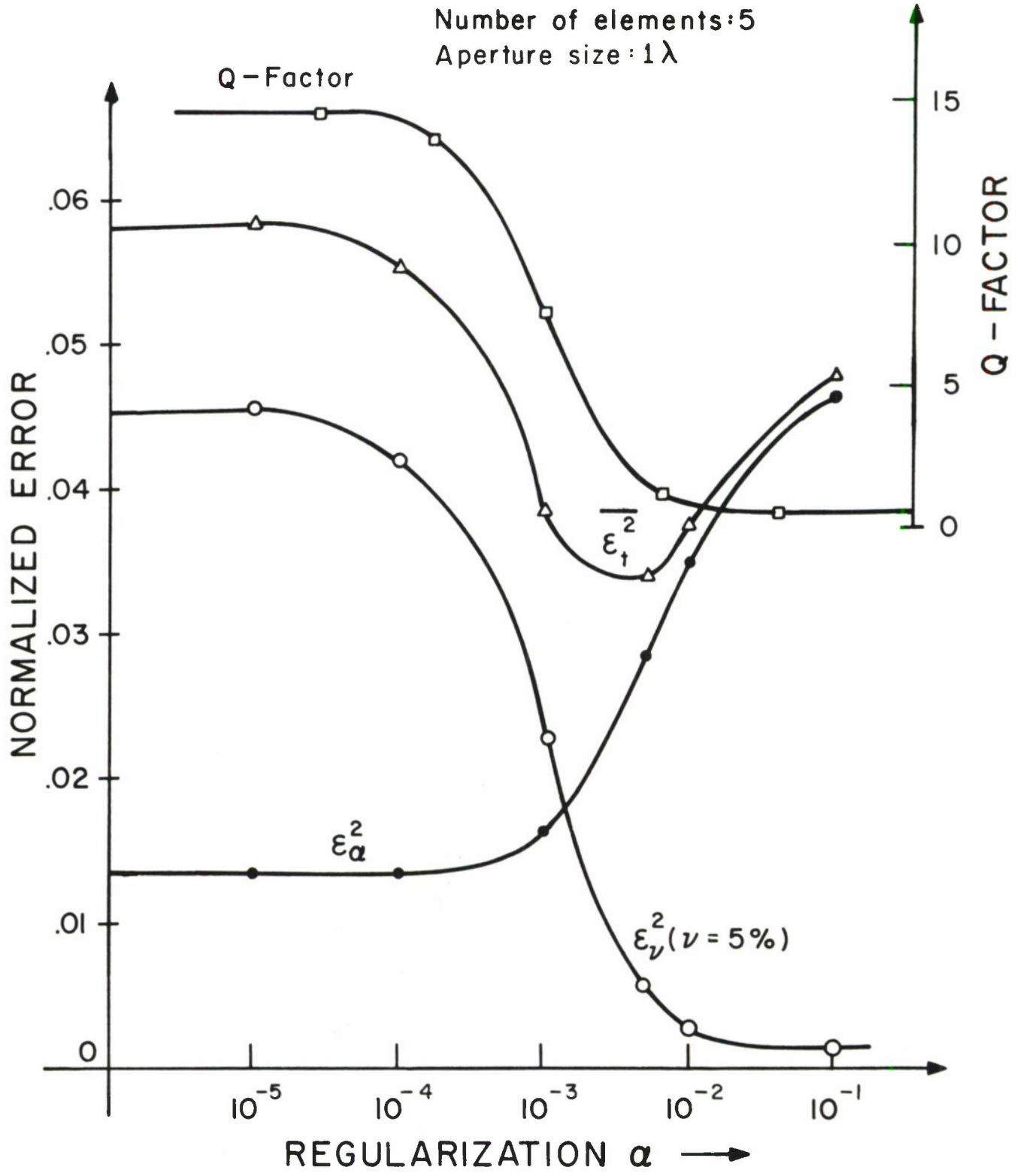

Figure 12. Error parameters ε_α^2, ε_ν^2, and $\overline{\varepsilon_t^2}$, and Q vs. regularization parameter α for the five-element array.

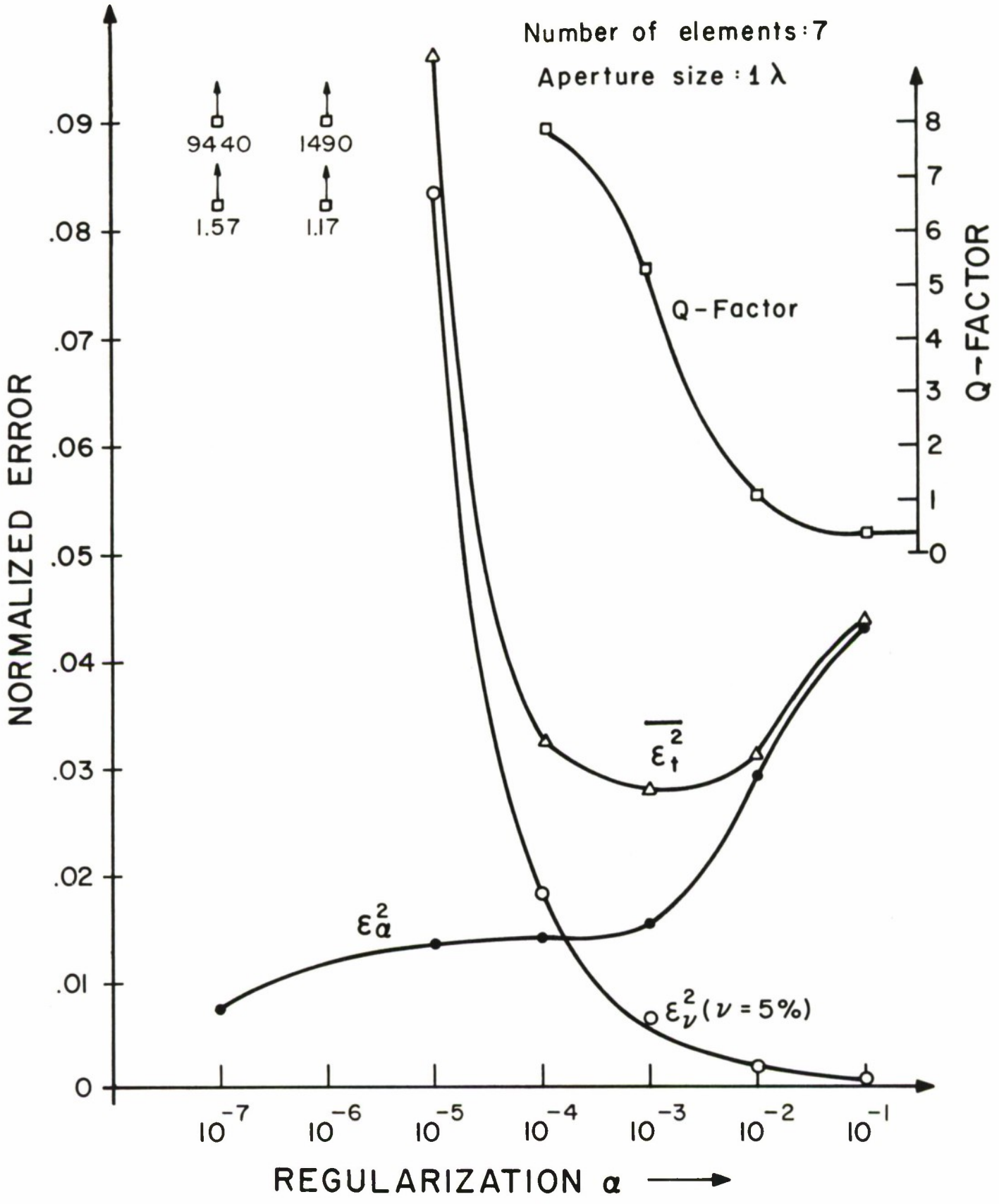

Figure 13. Error parameters ε_α^2, ε_ν^2, and $\overline{\varepsilon_t^2}$, and Q vs. regularization parameter α for the seven-element array.

From the far-field power pattern intensity $|\bar{g}_\alpha|^2$ in Figures 3 to 11, curves for the gain vs. solid angle, as described in the introduction, were derived. These curves are shown in Figures 14 and 15 for the five- and seven-element array, respectively, for the cases $\alpha = 0$ and $\alpha = 10^{-2}$. The gain curve for an elementary dipole is also shown for comparison. For example, in Figure 14, for a directive gain level of 0.8, the total solid angle in which the gain of each of the cases considered exceeds the 0.8 gain level is as follows:

Ideal isotropic radiator	:	4π
Five element array ($\alpha = 0$)	:	3.82π
Five element array ($\alpha = 10^{-2}$)	:	3.36π
Elementary dipole	:	2.72π.

A plot of $1/Q_\upsilon$ vs. $1/Q$ is shown in Figure 16.

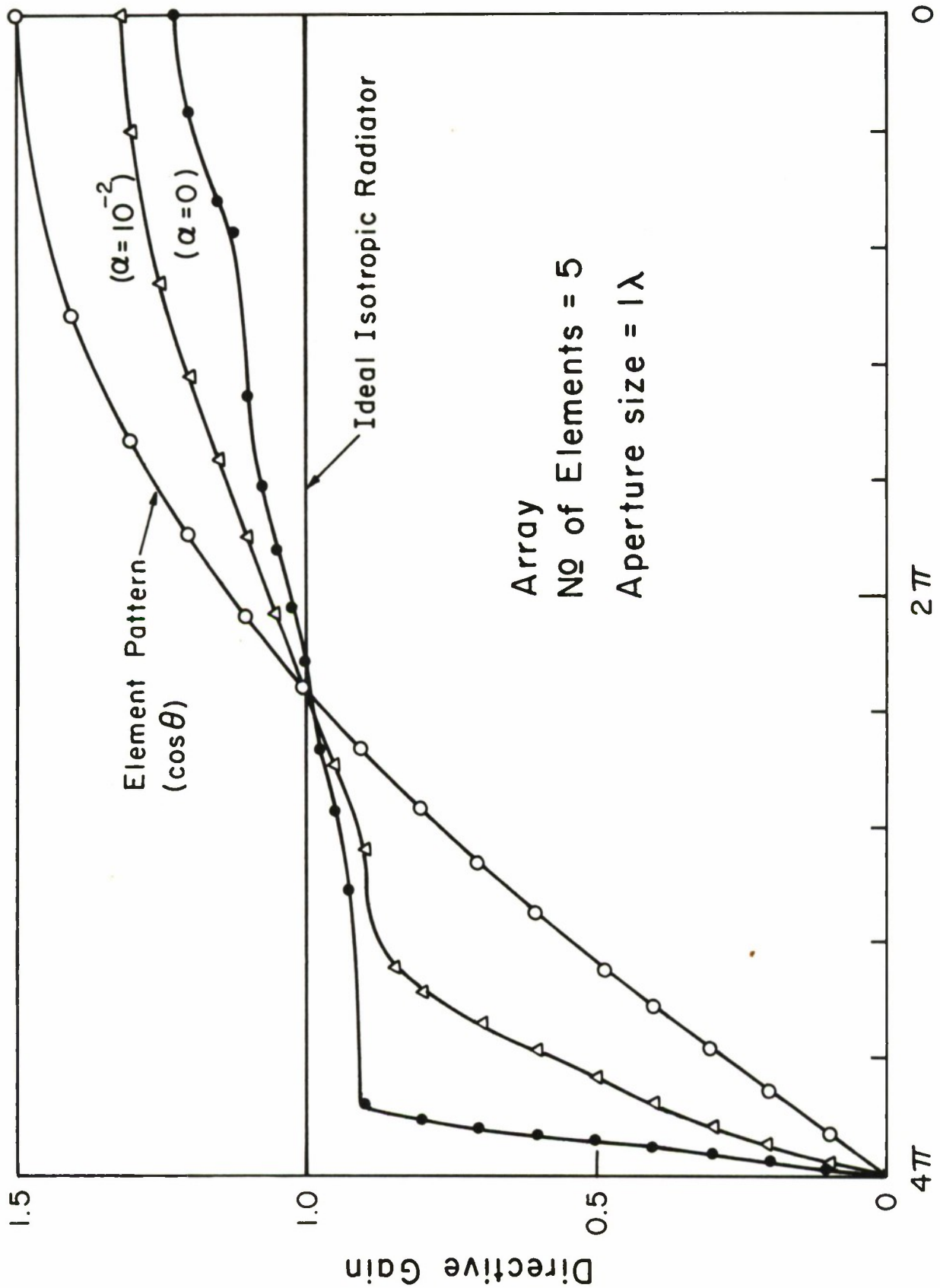

Figure 14. Gain vs. solid angle for the five-element array.

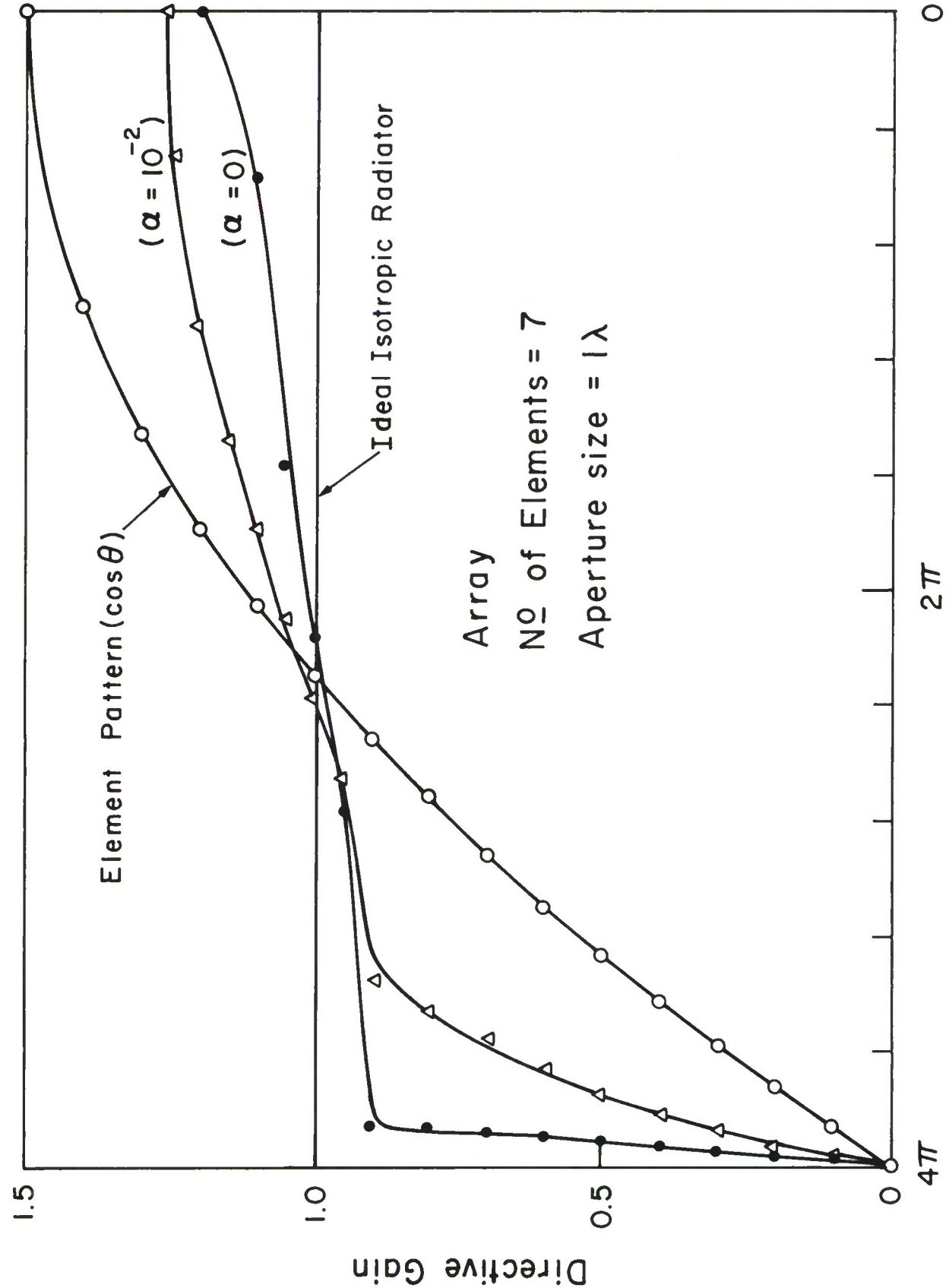

Figure 15. Gain vs. solid angle for the seven-element array.

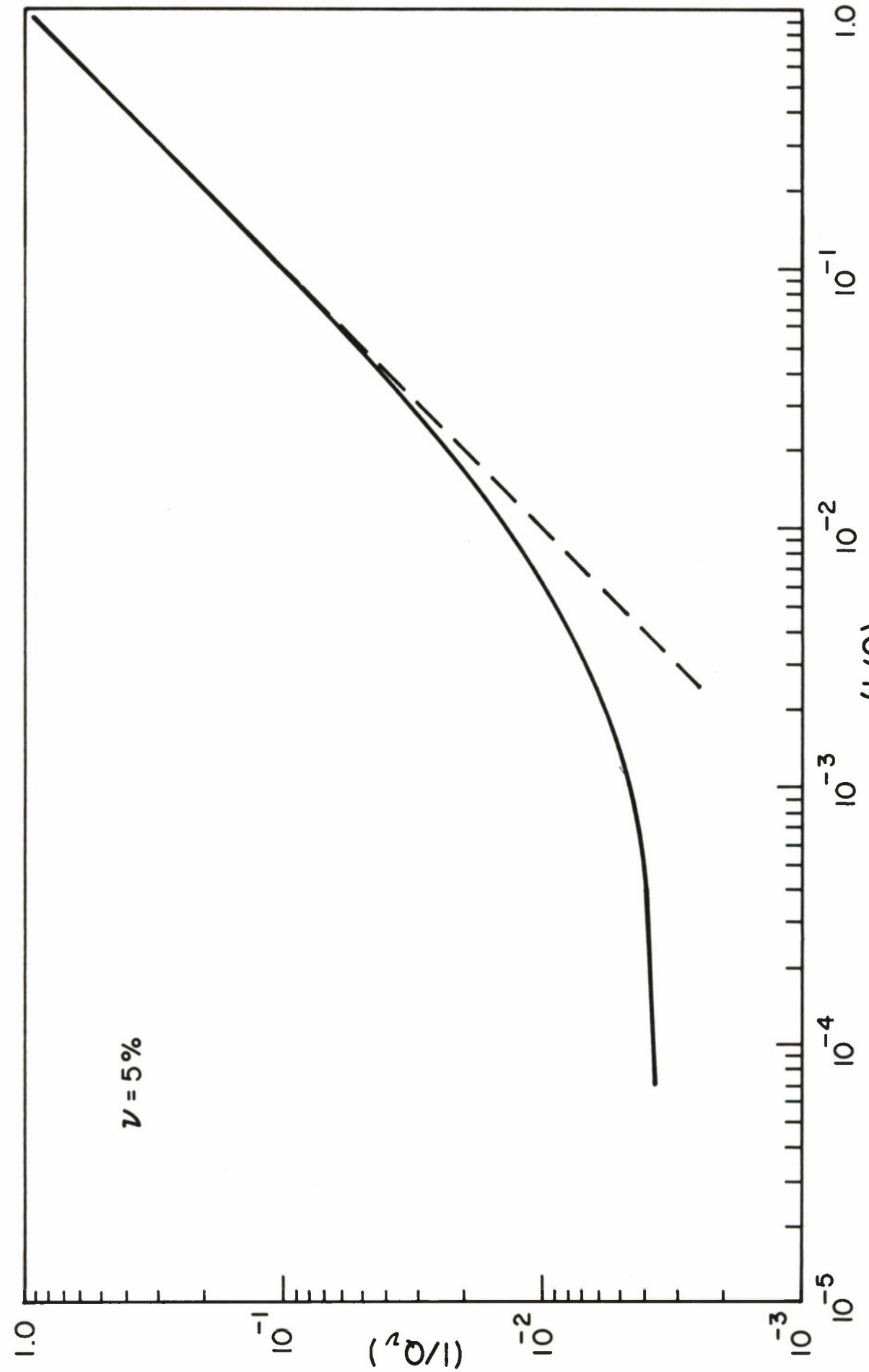

Figure 16. Plot of $1/Q_v$ vs. 1/Q for both five- and seven-element arrays.

5. COMMENTS ON THE NUMERICAL RESULTS AND THE CHOICE OF α

The first observation is that using an array does, indeed, improve the low gain performance. The gain curves in Figures 14 and 15 for $\alpha = 0$ come closest to that of an ideal isotropic radiator among all designs considered. Comparing the gain curves of the five-element to the seven-element array, only a slight improvement in low-gain performance is observed in the latter. The aperture size in both cases, however, is the same.

The performance of those designs corresponding to relatively small values of α looks, indeed, promising. However, in the presence of random errors in the currents, the performance of these designs deteriorates drastically, as shown in Figures 3 to 4 and 6 to 9. In such instances, a single element has a better performance than the array!

In deciding which value of α to use, it becomes imperative to study the behavior of the quantities ε_α^2, ε_ν^2, and Q. For a constant power radiated, the Q-factor is directly proportional to ohmic losses while the error ε_ν^2 is an indication of the sensitivity of the design to error. In Figures 12 and 13, as α approaches zero, ε_α^2 decreases, and both Q and ε_ν^2 increase. For the larger values of α, these trends are reversed. The design then must be a compromise between ε_α^2, ε_ν^2, and Q. A good compromise is that value of α which minimizes the total error $\overline{\varepsilon_t^2}$. For the five-element array, this corresponds to $\alpha = 3.54 \times 10^{-3}$, $Q = 2.25$, and $\varepsilon_\nu^2 = .008$ and, for the seven-element array, to $\alpha = 1.6 \times 10^{-3}$, $Q = 4.0$, and $\varepsilon_\nu^2 = .0045$. For these particular values of α, the seven-element array has larger ohmic losses, but is less sensitive to errors than the five-element array.

It is observed in Figure 16 that the introduction of random errors in the element excitations produces a decrease of the Q-factor, that is, an increase of the power radiated for a given norm of the sources. For values of Q less than 10, the reduction is very small. For values of Q larger than 10, the reduction becomes appreciable, and for values of Q larger than 10^4 Q_ν, becomes constant, equal to 270.

6. STATISTICAL ESTIMATION OF $1/Q_\nu$ AND ε_ν^2

The numerical determination of $1/Q_\nu$ and ε_ν^2, as outlined in the previous section, can be time consuming since the averages have to be taken over a large number of trials. It would be advantageous, therefore, if the quantities $1/Q_\nu$ and ε_ν^2 could be estimated analytically. From the expression for $f_{\alpha\nu}$ in Equation (16) and the definition of the L_2 norm in the space of aperture source functions given in Equation (5), the L_2 norm of $f_{\alpha\nu}$ is evaluated:

$$||f_{\alpha\nu}||^2 = \sum_{n=1}^{N} \bar{f}_{\alpha_n} \bar{f}_{\alpha_n}^{\,*} (1+\nu_n)(1+\nu_n^*),$$

and the expected value of this quantity is found to be

$$E\{||f_{\alpha\nu}||^2 = ||\bar{f}_\alpha||^2 (1+\nu^2)$$

where, for $\nu^2 << 1$

$$E\{||f_{\alpha\nu}||^2\} = ||\bar{f}_\alpha||^2. \tag{20}$$

The far-field pattern $g_{\alpha\nu}$, corresponding to an aperture source distribution $f_{\alpha\nu}$, is given by Equation (4):

$$g_{\alpha\nu} = \sum_{n=1}^{N} \bar{f}_{\alpha_n} (1+\nu_n) g_n(\xi).$$

From Equations (6) and (10), the L_2 norm of $g_{\alpha\nu}$ is evaluated,

$$||g_{\alpha\nu}||^2 = \sum_{n=1}^{N} \sum_{m=1}^{N} G_{nm} \bar{f}_{\alpha_n}^{\,*} \bar{f}_{\alpha_m} (1+\nu_n^*)(1+\nu_m),$$

and the expectation is found to be

$$E\{||g_{\alpha\nu}||^2\} = ||\bar{g}_\alpha||^2 + \nu^2 G_{00}||\bar{f}_\alpha||^2. \tag{21}$$

The expected value of $1/Q_\nu$ is defined to be

$$E\{1/\underline{Q_\nu}\} = E\{||g_{\alpha\nu}||^2 \,/\, ||f_{\alpha\nu}||^2\}.$$

However, Equation (20) shows that when the mean square level of error ν is small, the expected value $||f_{\alpha\nu}||^2$ may be approximated by $||\bar{f}_\alpha||^2$ and the following relation for $1/Q_\nu$ is obtained from Equation (21):

$$1/Q_\nu = E\{1/\underline{Q_\nu}\} \simeq 1/Q + G_{00}\nu^2. \tag{22}$$

Before computing the relative error ε_ν^2 due to random errors, $g_{\alpha\nu}$ should be normalized so that

$$E\{|\cdot|g_{\alpha\nu}||^2\} = ||\bar{g}_\alpha||^2.$$

From Equation (21), the normalization factor F is given by

$$F = [1+\nu^2 G_{00} Q]^{-1/2} = [Q \cdot E\{\frac{1}{\underline{Q_\nu}}\}]^{-1/2}. \tag{23}$$

Let $\bar{g}_{\alpha\nu}$ denote the normalized far-field pattern of the aperture sources in the presence of random error.

$$\bar{g}_{\alpha\nu} = F\, g_{\alpha\nu}.$$

The relative error ε_ν^2 is given by

$$\varepsilon_\nu^2 = E\{\underline{\varepsilon_\nu^2}\} = E\{||\bar{g}_{\alpha\nu} - \bar{g}_\alpha||^2\} \,/\, ||\bar{g}_\alpha||^2$$

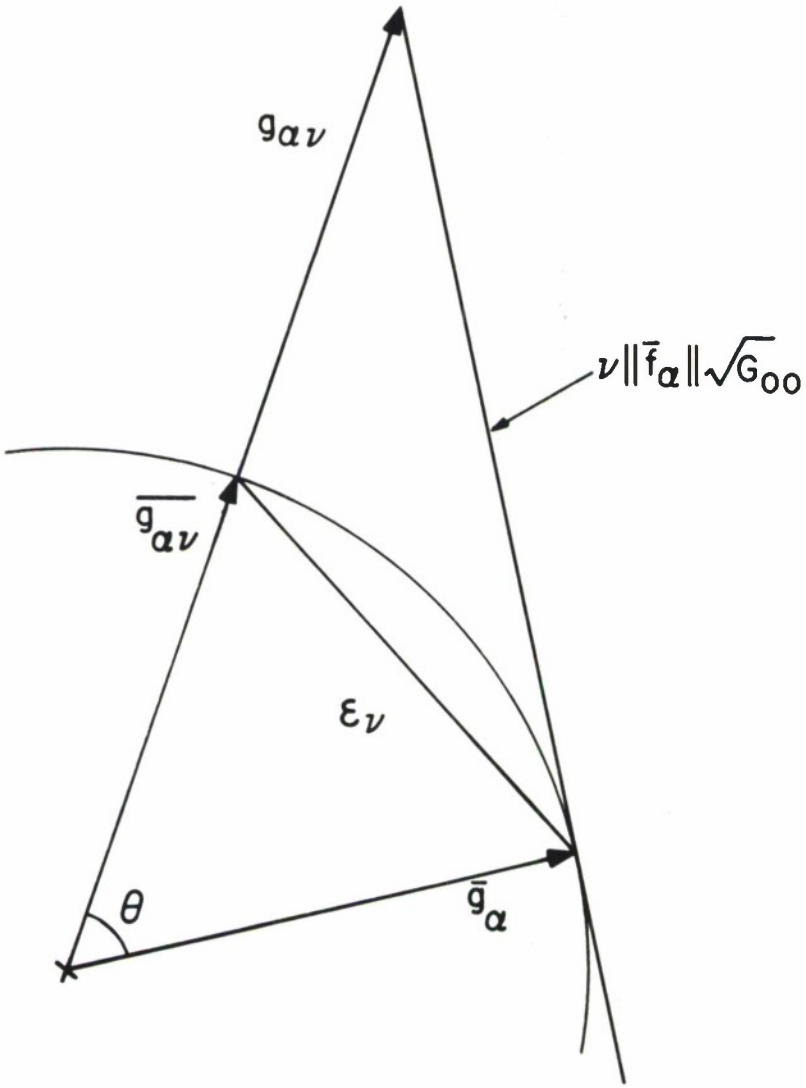

Figure 17. Schematic representation of the relationship between the pattern functions and the error parameters.

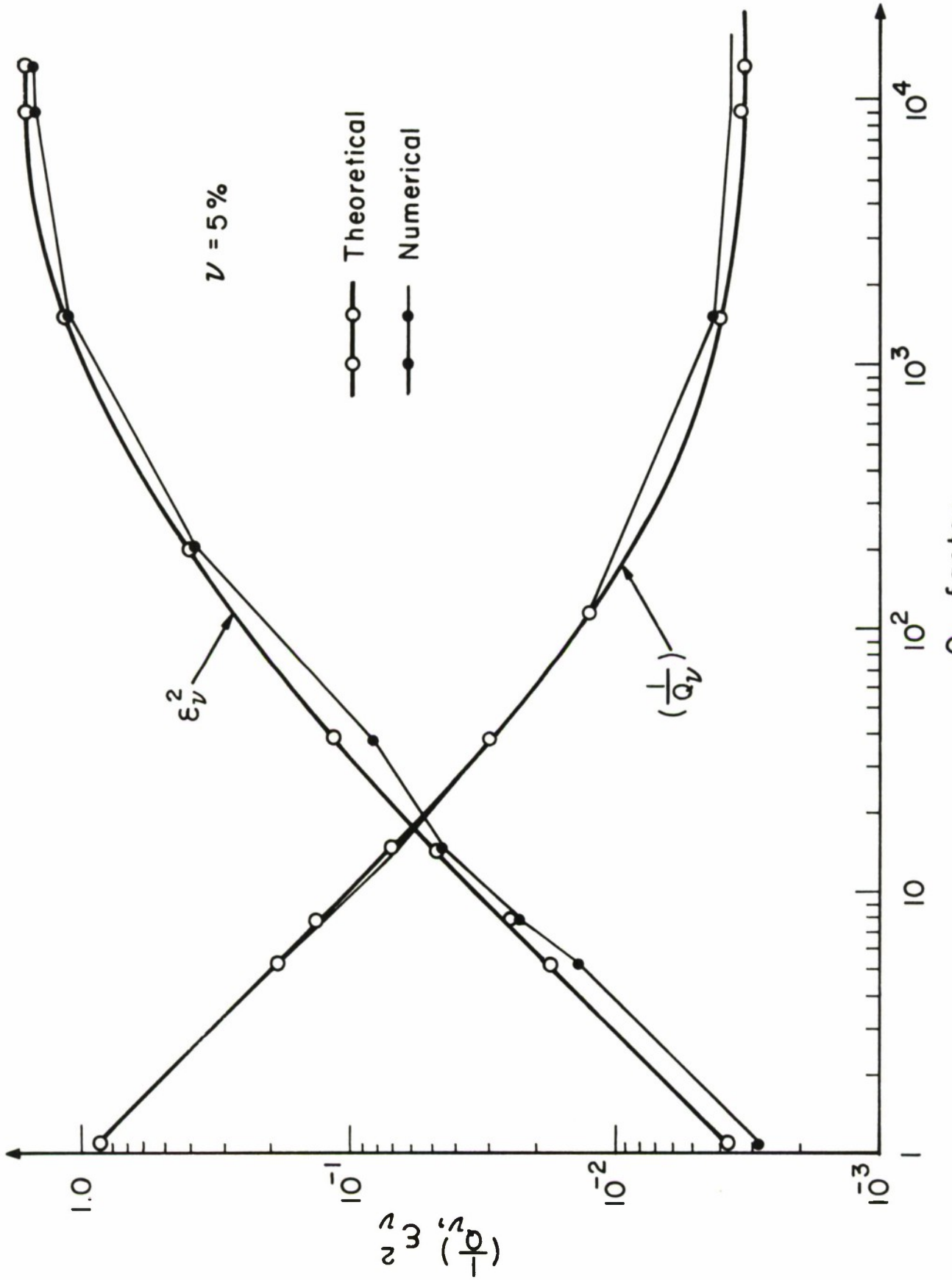

Figure 18. Plot of the theoretical and numerical values of ε_ν^2 and $1/Q_\nu$ vs. the Q-factor.

where

$$\bar{g}_{\alpha\nu} - \bar{g}_{\alpha} = \sum_{n=1}^{N} \bar{f}_{\alpha_n} g_n [F(1+\nu_n)-1].$$

Taking the norm and then the expectation, the following relationship is obtained for ε_ν^2:

$$\varepsilon_\nu^2 = 2(1-F). \tag{24}$$

This equation relates ε_ν^2 simply to the drop in the Q-factor when random errors are introduced in the sources.

Equation (24) can be rederived from the schematic representation in Figure 17. Equation (21) shows that the quantities $||\bar{g}_\alpha||$, $\nu||\bar{f}_\alpha||\sqrt{G_{00}}$, and $[E\{||\bar{g}_\alpha||^2\}]^{1/2}$ are related by the Pythagorean theorem. Therefore, the tangent of the angle θ shown in Figure 17 is given by

$$\tan\theta = \nu\sqrt{QG_{00}} \tag{25}$$

and

$$\varepsilon_\nu = 2 \sin\frac{\theta}{2}, \tag{26}$$

which can be rewritten in a form similar to that of Equation (24):

$$\varepsilon_\nu^2 = 2(1-\cos\theta).$$

Plots of $1/Q_\nu$ and ε_ν^2 as a function of Q calculated from Equations (22) and (24) are shown in Figure 18. The values of these quantities evaluated numerically are also shown for comparison. The agreement is very good.

7. CONCLUSION

A method has been outlined to design a linear array whose gain is close to unity and, therefore, whose pattern is nearly isotropic. Tihonov's regularization algorithm is used to produce a family of designs which depend on a parameter α.

It is found that as α approaches 0, the error ε_α^2 from the actual to the desired pattern decreases. But the norm $||f||^2$ of the aperture function, which for a unit power radiated is also the supergain ratio Q introduced by Taylor, increases. This is accompanied by an increase in the sensitivity of the design to errors represented by ε_ν^2. An acceptable design has to be a compromise between these three quantities.

Although the sensitivity to error varies in the same direction as Q, it is not directly proportional to it. A general relation has been established between these two quantities. This relation has been verified numerically and it provides a useful guide for choosing the amount of regularization.

The regularization method proves to be effective in designing nearly isotropic arrays of reasonable sizes.

REFERENCES

1. W. G. Scott and R. M. SooHoo, "A theorem on the polarization of null-free antennas," IEEE Trans. Antennas and Propagation, Vol. AP-14, pp. 587-590, September 1966.

2. A. N. Tihonov, "Solution of incorrectly formulated problems and the regularization method," Soviet Math., Dokl. 4, pp. 1035-1038, 1964.

3. H. S. Cabayan, G. A. Deschamps, and P. E. Mayes, "Stable numerical solutions to antenna synthesis problems," URSI 1969 fall meeting, pp. 38-39.

UNCLASSIFIED

Security Classification

DOCUMENT CONTROL DATA - R&D

(Security classification of title, body of abstract and indexing annotation must be entered when the overall report is classified)

1. ORIGINATING ACTIVITY *(Corporate author)*
Antenna Laboratory, Department of Electrical Engineering, Univ. of Illinois under Purchase Order No. CC-401 to M.I.T. Lincoln Laboratory

2a. REPORT SECURITY CLASSIFICATION
Unclassified

2b. GROUP
None

3. REPORT TITLE
LINEARLY POLARIZED ARRAYS WITH ALMOST ISOTROPIC RADIATION PATTERNS

4. DESCRIPTIVE NOTES *(Type of report and inclusive dates)*
Technical Report

5. AUTHOR(S) *(Last name, first name, initial)*
H. S. Cabayan
G. A. Deschamps

6. REPORT DATE	7a. TOTAL NO. OF PAGES	7b. NO. OF REFS
June 1970	45	3

8a. CONTRACT OR GRANT NO.	9a. ORIGINATOR'S REPORT NUMBER(S)
AF 19(628)-5167 b. PROJECT AND TASK NO. 627A c. Purchase Order No. CC-401 d.	Antenna Laboratory Report No. 70-10 9b. OTHER REPORT NO(S) *(Any other numbers that may be assigned this report)* ESD-TR-70-195 UILU-ENG-70-308

10. AVAILABILITY/LIMITATION NOTICES
This document has been approved for public release and sale; its distribution is unlimited.

11. SUPPLEMENTARY NOTES	12. SPONSORING MILITARY ACTIVITY
This work was partially supported by NSF Grant GK 2120	Air Force Systems Command, USAF

13. ABSTRACT

A linearly polarized antenna cannot radiate power uniformly in all directions. However, by controlling the aperture excitation, as is done in an array, it is possible to reduce the maximum gain and approach conditions for isotropic radiation. A numerical method is presented which generates a family of designs which depend on a parameter α. As α approaches zero, the radiation pattern tends to become more isotropic. However, the efficiency is reduced and the sensitivity of the pattern to errors in the aperture function is increased. In some cases this sensitivity is so high as to make the result worthless. The design, therefore, must be a compromise between closeness to conditions of isotropic radiation on one hand, and losses and sensitivity to errors on the other. The sensitivity to errors, expressed by the pattern deterioration for a given level of error, has been evaluated by a numerical experiment (Monte Carlo method). A general relation has also been established between the sensitivity and the losses in the antenna. It agrees with the numerical experiment and can be used as a guide to choose the regularization parameter α.

14. Key Words
Unity Gain Antenna; Linearly Polarized Arrays; Sensitivity to Error; Isotropic Radiation; Regularization; Synthesis; Arrays

DD FORM 1 JAN 64 1473

UNCLASSIFIED

Security Classification